Formation Factor Method

for the

In Situ prediction of Soil Properties

L. Segaran

Term Project

ECI 284 - Winter 2002

UC Davis

1. INTRODUCTION

ELECTRICAL CHARACTERIZATION OF TRANSVERSELY ISOTROPIC SANDS.

The Formation factor F, defined as the ratio of the conductivity of the fluid which saturates a sand aggregate to the conductivity of the mixture, is shown theoretically to depend on the basic features of the sand structure.

$$Formation\ \ factor,\ F = \frac{conductivity\ \ of\ \ the\ \ pore\ \ fluid}{conductivity\ \ of\ \ the\ \ sample}$$

May be measured in different directions.
F_H = horizontal formation factor
F_V = vertical formation factor

Average Formation Factor, $\overline{F}$

$$\overline{F} = \frac{F_V + 2F_H}{3}$$

For given sand the average formation factor, $\overline{F}$ is only a function of porosity and is independent of the orientation of particles for non-cemented soils. The average formation factor is related to porosity and the average shape factor $\bar{f}$, by the expression

$$\overline{F} = n^{-\bar{f}}$$

$\overline{F}$ and $\bar{f}$ are independent of particle orientation. An electrical index, A (the anisotropy index), quantifying the anisotropy of particles has been proposed by Arulanandan and Kutter (1978) as

$$A = \sqrt{\frac{F_V}{F_H}}$$

where F_V and F_H are the formation factors measured in the vertical and horizontal directions.

The three parameters $\overline{F}$, $\bar{f}$, and A can be used to characterize the porosity, the shape of particles, and anisotropy of particles. Using the results of the thin section studies made by Mitchell et al., 1976, the vertical and horizontal formation factors, and the anisotropy index of soil particles are predictable. Close agreement between the measured and predicted values of F_V, F_H, and A confirms the validity of the theoretical equations to characterize the structure of soils using the non-destructive formation factor method.

The derived properties of non-clay minerals are governed by the grain and aggregate characteristics of the particles and stress conditions. It has been shown that $\overline{F}$ is a unique function of porosity. The anisotropy index, A, quantifies particle orientation, and $\bar{f}$ is a measure of the shape of the particles. Thus $\overline{F}$ and A may be used to quantify the aggregate property which is sensitive to sample disturbance and needs to be measured insitu. Grain property (shape) is insensitive to sampling disturbances and can be determined on disturbed samples. It should therefore be possible to correlate certain soil properties such as stress ratio required to cause liquefaction versus number of cycles of loading and dynamic shear modulus with a combination of the parameters $\overline{F}$, A, and $\bar{f}$. Empirical correlation of this type could be extremely useful in evaluating the performance of sites which contain sand deposits subjected to earthquakes. Laboratory correlations between the electrical parameters and cyclic stress ratio required to cause liquefaction as a function of number of cycles of loading, the shear wave velocity, the shear modulus, the compression index, the hydraulic conductivity, the coefficient of earth pressure at rest, the critical state friction angle, and the in situ porosity are presented in the next section.

2 SOIL PROPERTIES USING THE FORMATION FACTOR METHOD

2.1 Porosity

Porosity has been shown theoretically to be related to the average formation factor, $\overline{F}$. To illustrate this, horizontal and vertical formation factor measurements were made in the laboratory on lucite balls and Monterey "0/30" sand samples, prepared by three different methods. Two 6 inch cubical cells, one with two 6 inch square platinum coated copper electrodes fixed on two opposing vertical faces, and the other with electrodes on top and bottom faces, were used for making horizontal and vertical electrical resistance measurements respectively (Arulmoli, Arulanandan and Seed, 1985). The $\overline{F}$ vs. porosity relationships obtained for all three methods of sample preparation were shown to be a function of porosity as presented in Figures 2.1 and 2.2 for lucite balls of 1/8 inch diameter and Monterey "0/30" sand respectively.

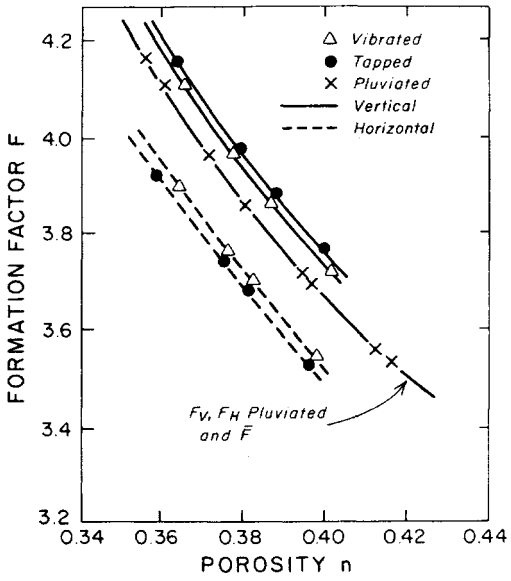

Figure 2.1
Vertical, Horizontal and Average Formation Factor versus Porosity Relationships for Lucite Balls Prepared by Three Different Methods

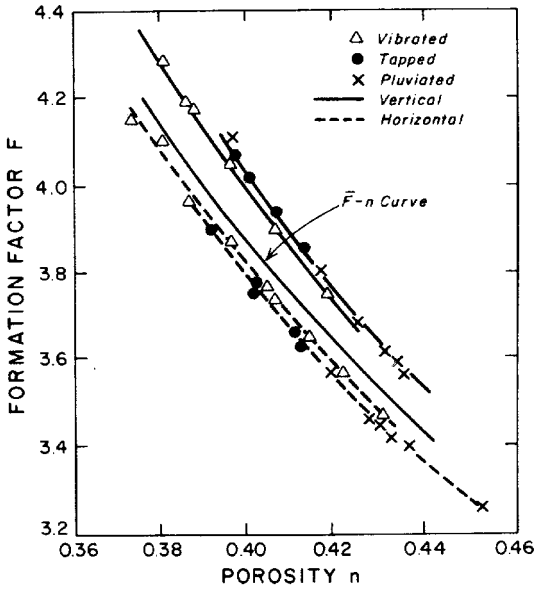

Figure 2.2
Vertical, Horizontal and Average Formation Factor versus Porosity Relationships for Monterey "0/30" Sand Prepared by Three Different Methods

Note that the samples were prepared in two separate cubical boxes and vibrated to different porosities with electrodes placed in the horizontal direction for F_V measurements in one box, and in the vertical direction for F_H measurements in the other box. As a result, the F_V and F_H values plotted in Figures 2.1 and 2.2 are at different porosities.

2.2 In Situ Determination of Stress Ratio Required to Cause Liquefaction as a Function of Number of Cycles of Loading and an Electrical Structure Index, $A^3/(\bar{F}\cdot\bar{f})$

To obtain a correlation between the cyclic stress ratio required to cause liquefaction in 10 cycles, $\tau_{c_{10}}$, and an electrical parameter, laboratory electrical measurements were made on reconstituted samples, for which the liquefaction characteristics have been extensively studied and reported by various investigators. It has been observed that $\tau_{c_{10}}$ increases with increasing $\bar{F}$ and $\bar{f}$, and decreases with increasing A and, further that the combination of $\bar{F}$, $\bar{f}$, and A which best correlates with stress ratio to cause liquefaction is $A^3/(\bar{F}\cdot\bar{f})$. The results are summarized in **Table 2.1**, and the correlation curve between $\tau_{c_{10}}$ and the electrical parameter, $A^3/(\bar{F}\cdot\bar{f})$, is shown in Figure 2.4.

Table 2.1
Electrical Measurements and Cyclic Stress Ratios to Cause Initial Liquefaction for Sands Tested

Sand type (1)	Method of preparation (2)	Porosity, n (3)	$\bar{F}$ (4)	A (5)	$\frac{A^3}{\bar{F}} \cdot \frac{1}{\bar{f}_m}$ (6)	τ_{c10} (7)	Investigator (8)
Monterey "0"	Dry pluviation	0.416	3.72	1.029	0.196	0.225	Mulilis et al. (28)
		0.395	3.94		0.185	0.306	
	Wet pluviation	0.416	3.72	1.026	0.194	0.250	
	Moist tamping	0.416	3.72		0.174	0.328	
				0.989			
		0.401	3.87		0.167	0.370	
Ottawa "C-109"	Dry pluviation	0.406	3.44		0.217	0.180	Harder Jr. (16)
		0.380	3.74	1.01	0.200	0.232	
		0.366	3.90		0.192	0.270	
		0.433	3.20		0.234	0.110	Finn et al. (14)
		0.401	3.48		0.215	0.180	
				1.01			
		0.383	3.71		0.202	0.225	
		0.375	3.80		0.197	0.286	
Sierra Diamond	Moist tamping	0.463	3.33	0.982	0.183	0.348	Arulmoli (7)
Lawson's Landing site	Wet pluviation	0.429	3.62	1.032	0.202	0.225	Arulmoli (7)
		0.419	3.74		0.195	0.270	
		0.412	3.82		0.191	0.325	
Reid Bedford site	Moist tamping	0.424	3.52		0.183	0.285	Townsend et al. (42)
				0.985			
		0.404	3.74		0.172	0.435	

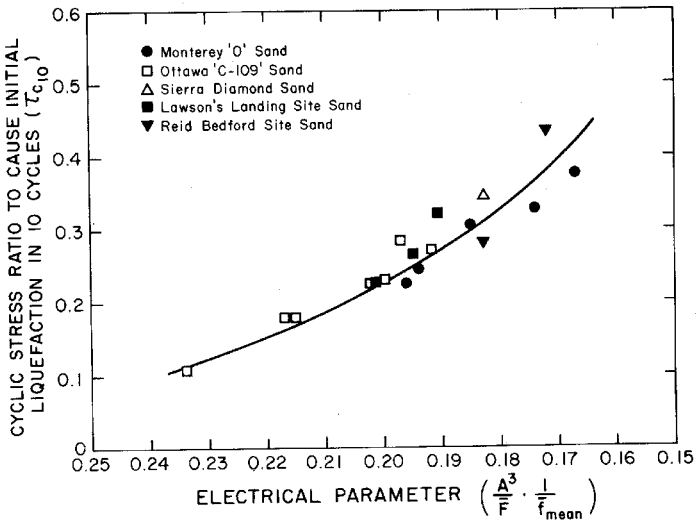

Figure 2.4
Laboratory Correlation Between Cyclic Stress Ratio Required to Cause Initial Liquefaction in 10 Cycles and Electrical Parameter, $A^3/(\bar{F} \cdot \bar{f})$

Similar correlations have been established for cyclic stress ratios to cause liquefaction in 5, 10, 15, 30 and 50 cycles (Arulmoli, 1982). These are shown in Figure 2.5.

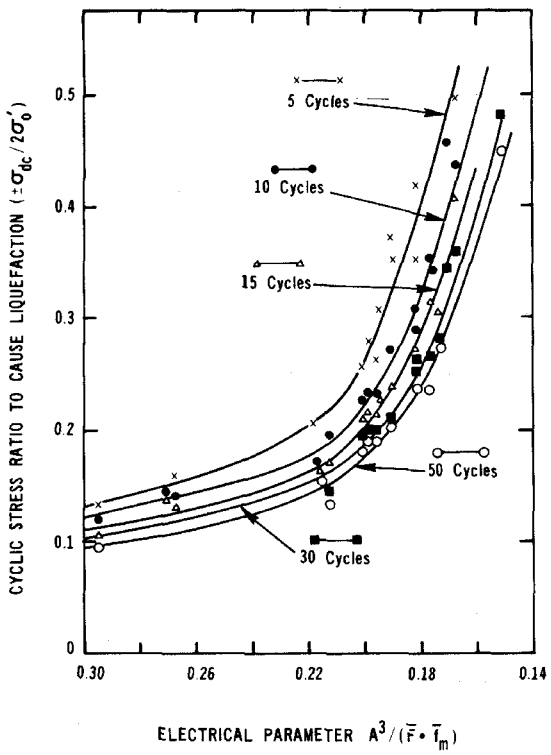

Figure 2.5
Laboratory Correlations Between Cyclic Stress Ratio to Cause Initial Liquefaction and Electrical Parameter, $A^3/(\bar{F}\cdot\bar{f})$

Using these correlations, the cyclic stress ratios were plotted against the number of cycles, N, for various values of the electrical parameter $A^3/(\bar{F}\cdot\bar{f})$, as shown in Figure 2.6.

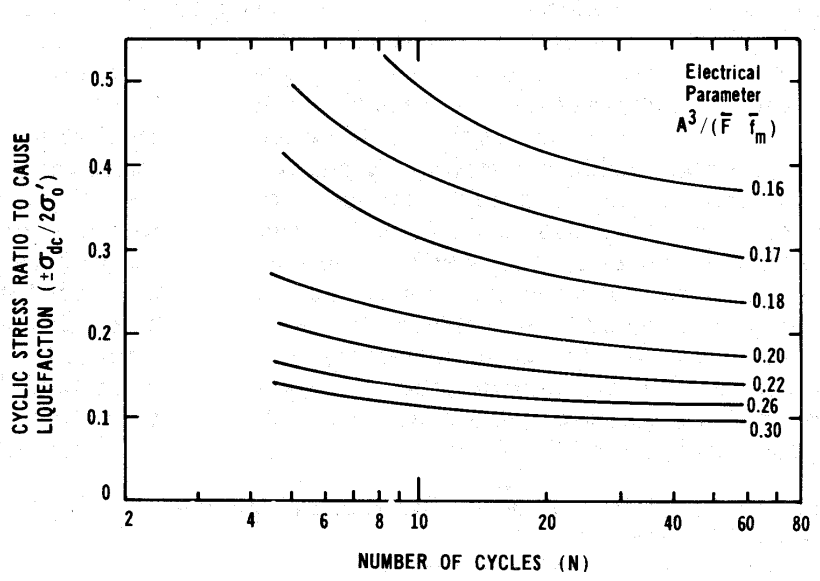

Figure 2.6
Correlation Between Cyclic Stress Ratio Required to Cause Initial Liquefaction and Number of Cycles for Different Values of Electrical Index, $A^3/(\bar{F}\cdot\bar{f})$

If $A^3/(\bar{F}\cdot\bar{f})$ can be obtained for a sand deposit, then the relationship between cyclic stress ratio to cause liquefaction and number of cycles can be established using the results shown in Figure 2.6.

The relationship between cyclic stress ratio versus number of cycles to cause initial liquefaction for the Monterey O sand prepared by different methods at the same porosity is shown in Figure 2.7.

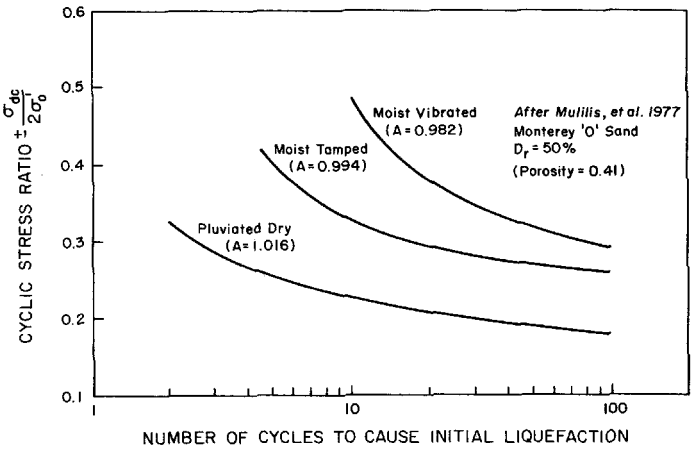

Figure 2.7
Cyclic Stress Ratio versus Number of Cycles to Cause Initial Liquefaction for Monterey 0 Sand Samples Prepared by Different Methods (after Mullis et al., 1977); Measured Electrical Anisotropy Index Values are after Arulanandan and Kutter (1978)

In Figure 2.7, σ_{dc} is the amplitude of deviatoric cyclic stress and σ'_0 is the initial effective confining pressure. Also given in Figure 2.7 are the measured electrical anisotropy index (A) values. It shows that for the same cyclic stress ratio, samples with a higher value of A need fewer cycles to cause initial liquefaction. This implies that, for a given number of cycles and given cyclic stress ratio, higher anisotropy produces a larger increase in pore-water pressure. Since the same sand with the same relative density was considered, $\overline{F}$ and $\bar{f}$ were constants for all three cases shown in Figure 2.7. Hence, an increase in A implies an increase in $A^3/(\overline{F}\cdot\bar{f})$ and an increase in pore water pressure.

A decrease in porosity, on the other hand, reduces the amount of settlement occurring for a given number of cycles and hence reduces the pore-water pressure generated in a given number of cycles. Also, a decrease in porosity increases $\overline{F}$ and hence decreases the index $A^3/(\overline{F}\cdot\bar{f})$.

Concerning the shape of particles, rounded particles are known to be more susceptible to pore pressure generation due to dynamic loadings than platy ones. Also,

rounded particles have a smaller $\bar{f}$ than platy particles and hence a larger value of $A^3/(\bar{F}\cdot\bar{f})$. These observations give qualitative justification for the parameter $A^3/(\bar{F}\cdot\bar{f})$ being correlated to properties associated with dynamic responses. The power 3 in the index shows the increased influence of anisotropy on dynamic properties.

In order to examine the validity of the electrical method to predict, in situ, the relationship between cyclic stress ratio to cause initial liquefaction and the number of cycles for soils, correlations obtained from laboratory cyclic tests conducted on undisturbed samples of sand obtained from the Niigata earthquake were compared with those predicted using electrical measurements on the same sample. Undisturbed samples were obtained by freezing the soil. A comparison of the results is shown in Figure 2.8.

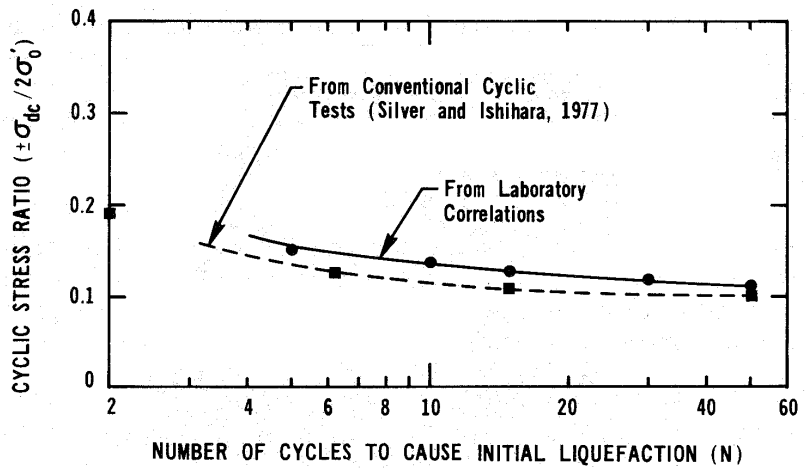

Figure 2.8
Comparison of Relationship Between Cyclic Stress Ratio to Cause Initial Liquefaction and Number of Cycles Obtained from Conventional Cyclic Tests and that Predicted from Electrical Measurements on Undisturbed Sand Samples from the Niigata Earthquake Area

The close agreement between the predicted and measured values provides justification for the use of this methodology for the in situ prediction of the relationship between cyclic stress ratio required to cause initial liquefaction and the number of cycles of loading.

2.3 Residual Friction Angle

By measuring the formation factors (vertical and horizontal) and porosity of a sand in the laboratory, one may obtain the average shape factor.

$$f_V = \frac{-\log F_V}{\log n}$$

$$f_H = \frac{-\log F_H}{\log n}$$

$$\bar{f} = \frac{f_V + 2f_H}{3}$$

Knowing $\bar{f}$, the slope of the critical state line (M) in q – p space is obtained from the follwing correlation (Arulanandan, et al., 1994)

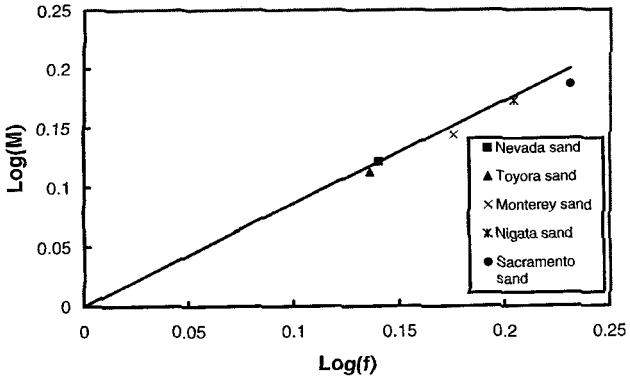

Figure 2.9
Relationship Between the Average Shape Factor and the Slope of the Critical State Line (M) in q – p Space

Moreover, from

$$M = \frac{(6\sin\theta)}{(3-\sin\theta)}$$

one may obtain the critical state friction angle, θ.

2.4 Hydraulic Conductivity

Specific surface area of sands can be obtained from the grain size distribution as shown in Figure 2.10 (Arulanandan and Muraleetharan, 1988).

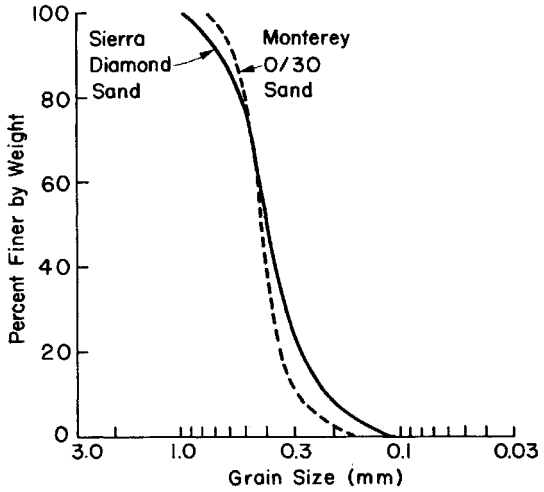

Figure 2.10
Particle-Size Distribution Curves for Sierra Diamond and Monterey 0/30 Sands

The specific surface area given as surface area per unit volume of soil particles may be calculated as follows.

$$SSA = \frac{6 \cdot \left[\left(\frac{W_1}{d_1} \right) + \left(\frac{W_2 - W_1}{d_2} \right) + ... + \left(\frac{100 - W_{n-1}}{d_n} \right) \right]}{100}$$

where W_1, W_2, …..etc, are the percentages passing; and d_i is the average diameter between W_i and W_{i-1}.

Once the porosity (obtained electrically via the formation factor method) and the specific surface area as defined above are known for sands, the Kozeny-Carman equation may be used to calculate hydraulic conductivity. By solving for the hydraulic

conductivity and substituting in known electrical parameteters for porosity, we obtain the following electrical index directly proportional to hydraulic conductivity

$$\frac{F^{-3/\bar{f}}}{\left(1-F^{-1/\bar{f}}\right)^2 (SSA)^2}$$

Arulanandan and Muraleetharan, 1988, have shown the linear relationship between hydraulic conductivity and the electrical index above as seen in Figure 2.11.

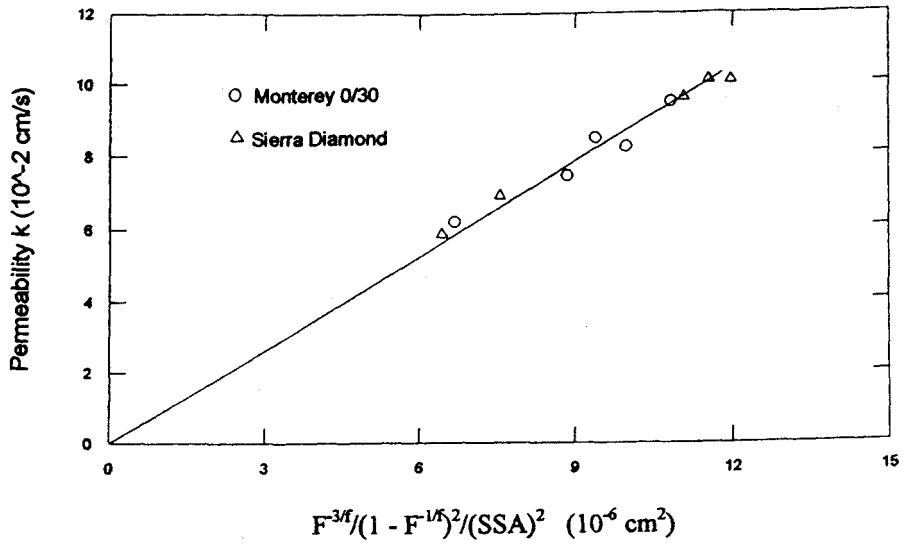

Figure 2.11
Correlation between Vertical Hydraulic Conductivity of Sands and Silty Sands and the Electrical Index $\dfrac{F^{-3/\bar{f}}}{\left(1-F^{-1/\bar{f}}\right)^2 (SSA)^2}$

2.5 Shear Modulus

One way of predicting maximum shear modulus, G_{max}, is by measuring the in situ shear wave velocity, V_S, and using

$$G_{max} = \rho V_S^2$$

in which ρ is the mass density of the deposit at the depth of measurement. Investigations have shown that the maximum shear modulus values for sands are strongly influenced by the confining pressure and the void ratio (Hardin and Drenevich, 1970; Seed and Idriss, 1970). A relationship between shear modulus, G, in pounds per square foot, and mean effective confining pressure, σ'_m, in pounds per square foot, was given by Seed and Idriss, 1970, as

$$G = 1000 \cdot K_{2_{max}} (\sigma'_m)^{1/2}$$

In the above equation, $K_{2_{max}}$ depends largely on the void ratio, the age of the deposit and in situ stresses (Seed and Idriss, 1970). A correlation between $K_{2_{max}}$ and an electrical parameter, $\overline{F}/(A \cdot \bar{f})^{1/2}$, was developed using measurements made both in the laboratory and in the field (Arulanandan et al., 1982). Field shear wave velocity measurements were made using cross hole seismic methods; the electrical measurements in the field were made using an electrical probe, which is described below. The correlation is shown in Figure 2.12.

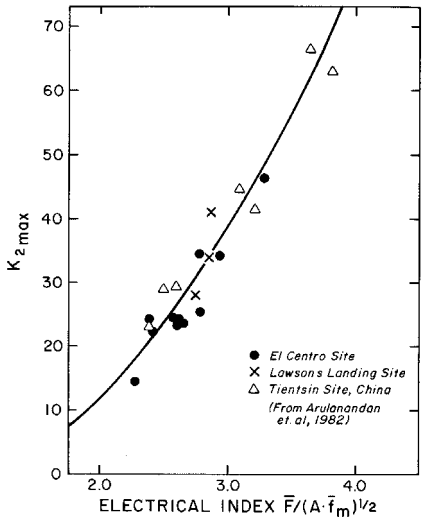

Figure 2.12

Correlation between K_2 max and Electrical Parameter, $\bar{F}/(A\cdot\bar{f})^{1/2}$

2.6 Compression Index, C_C, and Swelling Index, C_S

A correlation between the compression index (C_C) of sands (i.e., non-clay minerals) and the electrical index $A\bar{f}/\bar{F}$, which is a polynomial of degree 2, is given in Figure 2.13 (Harvey, 1981).

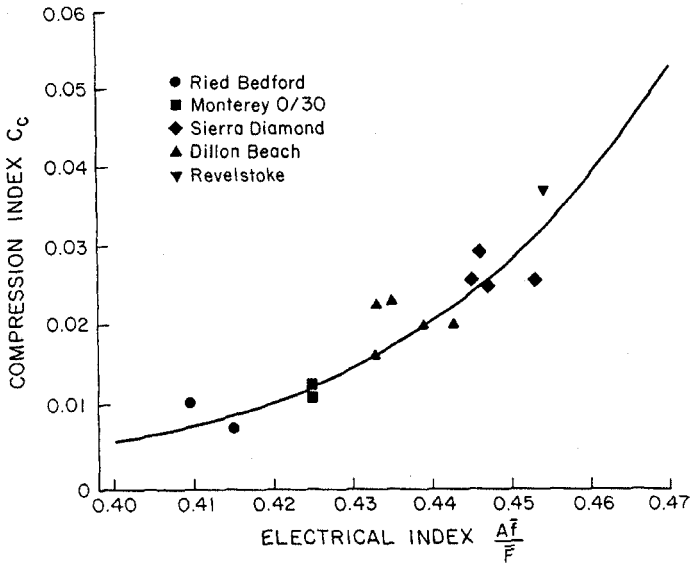

Figure 2.13
Correlation Between Compression Index and Electrical Index $A\bar{f} / \bar{F}$ for Sands (after Harvery, 1981)

Since the compression index of a sand is known to be influenced by the initial void ratio, it follows that the average formation factor ($\bar{F}$) calculated using the initial porosity should be included in the correlation. This correlation is valid up to a vertical effective stress of 5,500 lbf/sq ft. An approximate estimate of the swelling index (C_S) may be possible by assuming $C_S = (1/4)C_C$.

The use of electrical parameters in evaluating porosity, the cyclic stress ratio required to cause liquefaction, and the shear wave velocity can only be realized if the in situ meausurement of $\bar{F}$, A and $\bar{f}$ is possible. Actually, since $\bar{f}$ can be obtained from the $\bar{F}$ - n relationship, independent of aggregate properties and thus sample disturbance, it can be measured from laboratory tests of disturbed samples. $\bar{F}$ and A depend on aggregate properties and should be measured in situ. An electrical formation factor probe that can be used to measure the electrical parameters in situ is described below.

2.7 The Coefficient of Lateral Earth Pressure at Rest, K_0

Anisotropic constitutive models (Anandarajah et al., 1984, Pietruozczak and Mroz, 1983) show that the coefficient of lateral earth pressure at rest, K_0, is a function of fabric friction (since clay structure is viewed as the cluster concept, it is more appropriate to use the term "fabric friction") and fabric anisotropy. It is impossible for frictionless material to develop any fabric anisotropy. On the other hand, if there is no fabric anisotropy (i.e. isotropic), it can be shown from any isotropic constitutive model that K_0 is a function of the angle of internal friction, ϕ', which is a measure of fabric friction. The anisotropy index, A, is an indirect measure of fabric anisotropy. Anandarajah et al., 1982 and Arulanandan et al., 1983, quantified fabric friction in terms of electrical parameters; and since K_0 is a function of fabric anisotropy and fabric friction, it is possible to develop a correlation between K_0 and electrical parameters as shown in Figure 2.14.

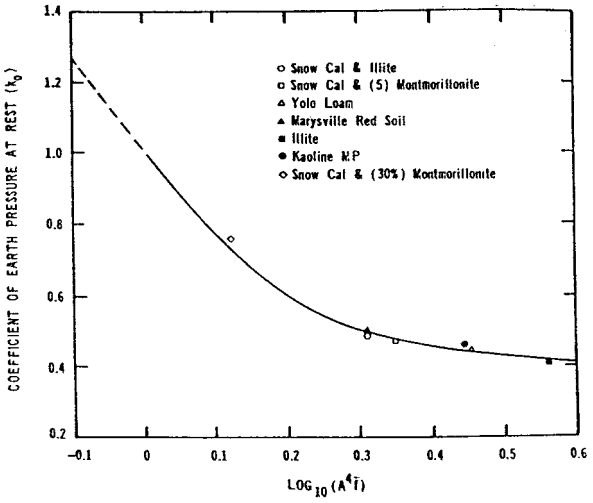

Figure 2.14
The Relationship Between the Coefficient of Lateral Earth Pressure at Rest and the Electrical Index, $A^4\bar{f}$ (Meegoda and Arulanandan, 1986)

Figure 2.14 is derived for clay soils. While Figure 2.14 has been used successfully for sands when obtaining K_0 for predicting earthquake simulation of liquefaction induced deformation, further work is needed to show the correlation between K_0 and the electrical parameters for sands.

In developing Figure 2.14, when there is no friction or anisotropy, K_0 is assumed as 1 and the lower limit of K_0 for fine grained soils is assumed as 0.38. The higher power of A in the electrical index $A^4\bar{f}$ demonstrates the heavy dependence of fabric anisotropy on K_0.

3. IN SITU FORMATION FACTOR PROBE

An electrical formation factor probe shown in Figure 3.1 can be used to make electrical measurements of soils in situ (Arulanandan, 1977).

Figure 3.1
GEOELECTRONICS Electrical Formation Factor Probe with Control Unit and Cable

The probe is capable of making measurements at any depth below the water table. The probe consists of three main parts.

the main body

A four foot long, three inch outside diameter steel tube houses electronics for the electrical bridge, and a 12 V gear pump to force solution into a water sampler cell which has electrodes for solution conductivity measurements.

probe tip

A 12 to 18 in long replaceable steel tube (3 in outside diameter and 1/16 in thick) is screw fitted to the above. The probe tip carries the electrodes for horizontal and vertical measurements. A schematic view of electrodes is shown in Figure 3.2.

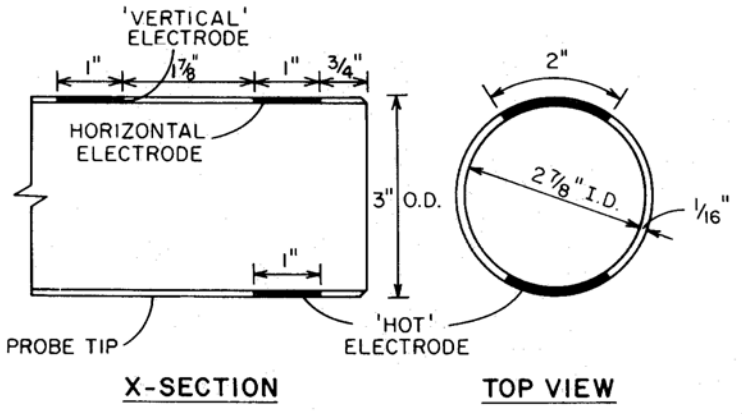

Figure 3.2
Schematic Views of In Situ Formation Factor Electrodes

The probe tip also carries a porous stone on its outside, about 4 in from the end, which is attached to one end of a thin metal tube, the other end of which is connected to the water sampler through the pump.

control unit

A microprocessor control unit for transmitting the electrical signal and receiving the measured electrical properties is connected to the electronics in the main body through a stiff cable.

The probe tip is connected to the main body and the assembly is dropped into a previously bored hole to the desired depth. The tip is pushed about 8 to 9 in into the soil so that the measurements can be made in the undisturbed region of soil. The area ratio is 8.9%, well below the minimum recommended by Hvorslev to achieve good results (Hvorslev, 1949). The setup is operated with a 12 V DC power source. The solution is

pumped from the saturated soil into the water sampler. The bridge impedance is varied in steps by the microprocessor, and the horizontal, vertical and solution resistances are obtained to an accuracy of about 1%. These results are used together with calibration curves for the vertical and horizontal electrodes and the water sampler, obtained from measurements in the laboratory. Vertical measurements are made at an angle and, by constructing a Mohrs circle of formation factors (similar to a Mohrs circle of stresses), the true vertical formation factor is obtained.

4. CONCLUSION:

1. Based on the electromagnetic theory applied to a granular two-phase material, the formation factor is rigorously shown to be a second order tensor whose first invariant is related to the porosity.
2. The principal values on this tensor are shown to characterize transversely isotropic symmetries of the granular structure based on statistical orientation of grains.
3. These properties of the formation factor can be used for an in situ determination of parameters associated with the constitutive modeling of soils. Such parameters are either initial values of state variables, or constants of constitutive models.

References:

1. K. Arulanandan "*SOIL STRUCTURE: In Situ Properties and Behavior*", Text Book ECI 283 (Draft)

2. Anandrajah, A., Arulanandan, K., Dafalias, Y. F., and Herrmann, L. R. (1982) "In-Situ Determination of Stress-Strain Relationships of Clays," International Symposium on Constitutive Laws for Engineering Materials: Theory and Applications, Tucson, Arizona, Jan. 10-14.

3. Anandarajah, A., Dafalias, Y. F., and Herrmann, L. R. (1984) "Bounding Surface Plasticity Model for Anisotropic Clays," Proceedings of the 5th ASCE-EMD Conference, University of Wyoming, Laramie.

4. Arulanandan, K., Anandarajah, A., and Meegoda, N. J. (1983) "Soil Characterization for Non-Destructive In-Situ Testing," Symposium Proceedings Part 2, The Interaction of Non-Nuclear Munitions with Structures, U.S. Air Force Academy, Colorado, pp. 69-75.

5. Arulanandan, K., Arulmoli, K., Dafalias, Y. F., and Herrmann, L. R. (1982) "In Situ Characterization of Saturated Sands and Silts for the Prediction of Dynamic Shear Modulus and Shear Wave Velocity," Department of Civil Engineering, University of California, Davis, California, Report to the Air Force Office of Scientific Research, Grant No. AFOSR-82-0216.

6. Arulanandan, K., and Kutter, B. (1978). "A directional structure index related to sand liquefaction," Proceedings of the Specialty Conference on Earthquake Engineering and Soil Dynamics, ASCE, Pasadena, California, pp. 213-230.

7. Arulanandan, K., and Muraleetharan, K. K. (1988) "Level Ground Soil Liquefaction Analysis using In-Situ Properties: I and II, "*Journal of Geotechnical Engineering, ASCE*, Vol. 114, No. 7.

8. Arulmoli, K., Arulanandan, K., and Seed, H. B. (1985) "New Method for Evaluating Liquefaction Potential," *Journal of the Geotechnical Engineering Division. ASCE*, Vol. 111, No. 1, pp. 95-114.

9. Li, X. S. (1997) "Modeling of Dilative Shear Failure," *Journal of Geotechnical Engineering, ASCE*, Vol. 123, No. 7, pp. 609-616,

10. Meegoda, N. J., and Arulanandan, K. (1986) "Electrical Method of Predicting In Situ Stress State of Normally Consolidated Clays," Proceedings of the In Situ 86', GT Division, ASCE, Blacksburg, Virginia, June 23-25, pp. 794-808.

11. Mulilis, J. P., et al. (1977) "Effects of Sample Preparation on Sand Liquefaction," Journal of the Geotechnical Engineering Division, ASCE, Vol. 103, No. 2, pp. 91-108.

12. Peitruszczak, St. and Mroz, Z. (1983) "On Hardening Anisotropy of K_0 Consolidated Clays," *International Journal for Numerical and Analytical Methods in Geomechanics*, Vol. 7, pp. 19-38.

13. Seed, H. B., and Idriss, I. M. (1970) "Soil Moduli and Damping Factors for Dynamics Response Analysis," *Report No. EERC 70-10*, University of California, Berkeley, California, December.

14. Verdugo, R. and Ishihara, K. (1996) "The Steady State of Sandy Soils," *Soils and Foundations*, Vol. 36, No. 2, pp. 81-91.

15. Wang, Z. L., Dafalias, Y. F. and Shen, C. K. (1990) "Bounding Surface Hypoplasticity Model for Sand," *Journal of Engineering Mechanics, ASCE*, Vol. 116, No. 5, May, pp. 983-1001.